

EDISON LIBRARY
DRI Ref No 111-72-18
Copy No. 1 of 1 copy.

Quarterly Technical Summary

Advanced Electronic Technology

15 November 1972

Prepared for the Department of the Air Force
under Electronic Systems Division Contract F19628-73-C-0002 by

Lincoln Laboratory

MASSACHUSETTS INSTITUTE OF TECHNOLOGY

LEXINGTON, MASSACHUSETTS



AD754945

ESD RECORD COPY

RETURN TO
SCIENTIFIC & TECHNICAL INFORMATION DIVISION
(DTI), BUILDING 1436

Approved for public release; distribution unlimited.

Quarterly Technical Summary

Advanced Electronic
Technology

15 November 1972

Issued 9 January 1973

Prepared for the Department of the Air Force
under Electronic Systems Division Contract F19628-73-C-0002 by

Lincoln Laboratory

MASSACHUSETTS INSTITUTE OF TECHNOLOGY

LEXINGTON, MASSACHUSETTS



Approved for public release; distribution unlimited.

The work reported in this document was performed at Lincoln Laboratory, a center for research operated by Massachusetts Institute of Technology, with the support of the Department of the Air Force under Contract F19628-73-C-0002.

This report may be reproduced to satisfy needs of U.S. Government agencies.

Non-Lincoln Recipients

PLEASE DO NOT RETURN

Permission is given to destroy this document
when it is no longer needed.

INTRODUCTION

This Quarterly Technical Summary covers the period 1 August through 31 October 1972. It consolidates the reports of Division 2 (Data Systems), Division 4 (Air Traffic Control) and Division 8 (Solid State) on the Advanced Electronic Technology Program.

Accepted for the Air Force
Joseph J. Whelan, USAF
Acting Chief, Lincoln Laboratory Liaison Office

CONTENTS

Introduction	iii
DATA SYSTEMS - DIVISION 2	
Introduction	1
Digital Computers - Group 23	3
I. Introduction	3
II. Integrated Circuit Processing	3
III. Photolithographic Interconnection of Plastic-Embedded Semiconductor Chips	4
IV. Testing and Mask Design	5
V. Applications and Mask Design	5
Computer Systems - Group 28	
I. Time-Shared Operations	9
II. Batch Operations	10
AIR TRAFFIC CONTROL - DIVISION 4	
Introduction	11
I. Summary	13
II. Approach and Landing Systems	13
III. Airborne Graphical Displays	17
SOLID STATE - DIVISION 8	
Introduction	19
Division 8 Reports on Advanced Electronic Technology	21
I. Solid State Device Research	27
II. Quantum Electronics	27
III. Materials Research	28
IV. Physics of Solids	28
V. Microelectronics	28

DATA SYSTEMS DIVISION 2

INTRODUCTION

This section of the report reviews progress during the period 1 August through 31 October 1972 on Data Systems projects funded by the Air Force. Separate reports on Speech, Seismic Discrimination, Educational Technology, Radar Measurements, and ATC Surveillance/Communication Analysis and Planning describe the work of Division 2 on other programs.

M. A. Herlin
Acting Head, Division 2
I. L. Lebow
Associate Head

DIGITAL COMPUTERS

GROUP 23

I. INTRODUCTION

The full complement of processing techniques required for fabricating high-speed bipolar integrated circuits (ICs) including buried As collectors, epitaxy and double-level metal will be operational by the first of the year, when first samples of the array multiplier chips (2 bit-gated adder) are due. Table 2-I shows the status of various circuits in design or fabrication.

TABLE 2-I STATUS OF LARGE-SCALE INTEGRATED DIGITAL CIRCUITS	
Circuit	Status
3-input gate	Production
16-transistor geometries	First working circuits
Double-level metal	First working circuits
Gate chain	Mask-making completed
2-bit adder	In process
A/D converter	Circuit design - mask design
C-circuit } Bit pipeline }	Circuit design
Basic arbiter	Experimental and theoretical evaluation
Error corrector	Logic design and statistical analysis
Submicron devices	Alignment and resolution

II. INTEGRATED CIRCUIT PROCESSING

A. Integrated Circuit Fabrication

The epitaxial reactor is now being brought on stream, and future epitaxial films will be produced in-house using As-buried collectors. This will enable faster turn-around time for new chip types and faster devices due to thinner collectors.

The first run of the 16-transistor test chip has been completed, including the successful etching of 0.05-mil geometry (compared with our normal 0.1-mil geometry) test transistors.

B. Computer Modeling

A film is being made which illustrates the operation of the semiconductor fabrication simulation system.

C. Metalization

Several runs of Al double-layer metalization have been completed. Depositions of oxide from the reaction of silane and oxygen at 450°C are used as the insulation. The layer-to-layer integrity has been very good with breakdown voltages of 400 to 600 V and leakage currents less than 1 nA. High contact resistance between metal layers at the via openings has been a problem. One solution is a final sinter temperature of 500°C after the second level metal has been patterned. We are currently looking at methods for reducing this high temperature to avoid metalization shorting out the shallow emitters.

Initial work has begun on a double-layer metalization scheme substituting Mo for Al. Its use could potentially avoid many problems, such as electromigration and emitter shorting.

D. Photolithography Techniques

The photoresist-etching processes for oxide cuts are now standardized and are adequate for making 0.05-mil (12,000-Å) openings in the case of a 16-transistor test wafer.

Considerable attention has been given to problems associated with metal etching. Thin photoresist on AlSi opens up at the top edges of metalized oxide cuts, permitting the conductors to be etched open. Higher viscosity resist eliminates this effect, but light reflected from the somewhat rough aluminum during exposure polymerizes the resist where narrow cuts are to be made and thus limits the narrowest resist opening to 0.15 mil. This problem has been solved by improving the collimation of the exposure source and compensating the dimensions of the mask. This combination permits 0.05-mil openings in the thicker resist-on-metal configuration. A second problem of marginal resist-to-metal adhesion has been solved by use of a silane metal treatment prior to resist application.

E. Electron-Beam Experiments

Lines of micron dimensions have been exposed by the electron beam in polymethyl-methacrylate resist. Utilizing this as a mask on oxide-covered silicon wafers, we have chemically etched the SiO₂ to linewidths (at the SiO₂ - Si interface) of 0.25 to 2.5 μm. Using this technique, we are attempting to diffuse emitter junctions through such lines to produce active transistors.

III. PHOTOLITHOGRAPHIC INTERCONNECTION OF PLASTIC-EMBEDDED SEMICONDUCTOR CHIPS

A. Single-Chip Memory Experiments

Twelve single-chip memory arrays have been constructed using Intel's IC memory chip 3101A. Each array has been operated in a dynamic pattern-cycling mode for at least 24 hours without failure. A 12-socket tester is being constructed so that all units can be simultaneously operated to acquire life-test data while larger memory arrays are being constructed.

B. Sensitizing Plastic Surfaces for Electroless Metal Deposition

A method for sensitizing thermosetting plastic surfaces for electroless metal deposition which does not use an acid oxidizing medium has been developed. This method binds sensitizing

metal hydrosols ($\text{PdO} \cdot \text{H}_2\text{O}$ or $\text{SnO} \cdot \text{H}_2\text{O}$) through a chelating silane coupling agent (ethylene-diamine propyltrimethoxy silane). The method works, but the electrodeposited metal does not appear as smooth, nor does it adhere as well as when the plastic is subjected to the oxidizing acid treatment.

IV. TESTING AND MASK DESIGN

A. Integrated Circuit Tests

Propagation delay measurements on the first run of 3-input gate ICs yielded 1.6-nsec average delay per gate for the 0.1-mil geometry gate and 2.8-nsec delay per gate for the 0.2-mil geometry gate. This compares with 2.7 nsec per gate for MECL 10,000 gates in a similar circuit.

It is expected that considerable improvement can be obtained when all processing parameters are optimized.

B. Transistor Performance Measurements

Computer programs, which measure and plot the base resistance r_b' and collector capacity C_c , and current gain as a function of collector current, are operational for the TIC terminal. Both can provide a family of curves for three specified collector voltages on a linear or logarithmic current scale. A program which plots diode capacity as a function of applied voltage and uses this data to provide a curve of doping density as a function of distance from the junction has also been tested. It is now being evaluated in conjunction with a Hg-tip wafer probe and, if operation is satisfactory, it will be used to make measurements on epitaxial wafers.

C. Evaluation of 16-Transistor Test Group

Initial transistors have been fabricated from the 16-transistor set and performance is encouraging. These initial devices have back collector contacts. They are temporarily being packaged in TO-18 headers since the tooling for the TO-51 package is not completed. Table 2-II compares the geometry of two transistor types which have been evaluated.

Parameter measurements on these initial devices are shown in Table 2-III.

The Q11 is a reference transistor. The other 14 devices, which have various geometry variations, will be compared with the Q11 in performance.

V. APPLICATIONS AND MASK DESIGN

A. Single Error Correction for Computer Memories

An investigation was made into the improvement in yields of integrated memory devices that could be achieved if a single error correcting capability were available, allowing the use of partially defective devices. A mathematical formula was developed for determining whether a single error correcting capacity would be useful, given the following parameters: the number of storage cells per integrated device, the average number of defective cells per device, the total word length, the number of digits of a word on a single device, and the number of devices in a manufacturing run. The formula was checked by a Monte Carlo computer simulation and found accurate. A typical result is that a yield of 50 percent can be achieved for the following

Division 2

TABLE 2-II
TRANSISTOR GEOMETRIES
(Measurements in mils)

	Q11	Q14
Buried N+	0.8×0.9	0.4×0.45
Collector	1.6×1.7	1.2×1.25
Base insert	0.1×0.6	0.05×0.3
Base	0.8×0.5	0.3×0.4
Emitter	0.1×0.6	0.05×0.3
Base-emitter stripe separation	0.1	0.5
Collector contact	0.2×0.8	0.1×0.4
Collector contact to base separation	0.2	0.15

TABLE 2-III
TRANSISTOR PARAMETER MEASUREMENTS

	Q11	Q14
Peak f_T (GHz) at $V_{cb} = 0V$	2.6	1.5
I_c (mA) for peak f_T	3.0	0.64
I_c (mA) for $f_T = 1$ GHz (low)	0.13	0.10
I_c (mA) for $f_T = 1$ GHz (high)	9.0	1.9
r_b^t (ohms minimum) at $V_{cb} = 0V$	95	155
I_c (mA) for minimum r_b^t	4.8	1.1
DC current gain at $V_{cb} = 1V$, $I_c = 1$ mA	180	40

parameters: 4096 storage cells per device, 17 defective cells per device (average), 64 digits per word, 4 digits of a word per device, 1000 devices in a manufacturing run. Under these conditions the yield of perfect devices is $e^{-17} = 0.4 \times 10^{-7}$.

The tacit assumption that defects in digits of the same word on the same device are independent is reasonable if the cells storing those digits are physically distant. For instance, the typical device described above could be organized into quadrants, each containing one of the digits.

A logical design for implementing a single error corrector has been devised. Its great regularity would allow it to be implemented almost entirely with repetitions of the same basic circuit.

B. Double Raster Display System

One major part of the Double Raster Display System hardware, the C4 computer, is now operational. C4 is a 32-bit, medium speed, Lincoln Laboratory built machine, that will process commands and manipulate raster picture bits of the Double Raster Display System. Checkout of the remaining hardware for the system will begin shortly.

C. C4 Computer Software

A series of diagnostic programs has been written for the C4 computer. The programs were designed to help pinpoint any hardware failures that might occur. In addition, a short program is being written to run with the daily TX-2 diagnostics. If any failures are detected by this program, the larger series of diagnostics will be run to determine the precise problem.

D. Logic Design Graphics System

A graphics system for logic design is being prepared on the 360/67 for general use. It is hoped that the system will be usable directly with any graphics device, including ARDS, Calcomp, SC-4060, and the TSP, when it becomes available; the system itself will be able to handle any device without concern by the user.

The system was based on the OLLS system now in use on a 2250 at the Draper Laboratory, and adapted for the environment at Lincoln Laboratory. In light of the requirement for different device applications, it was decided that the data base should be stored in text form on the 360/67, using the CMS file handling routines.

There are two basic functions of such a graphics system: (1) to produce drawings using subpictures and connections, and (2) to make available to the user a logic analysis of the behavior of the structure represented by the drawing. At this stage, the system will produce, modify, and store drawings in a drawing library, or data base, on the 2741 typewriter terminal; the picture-making function is complete except for the modules which handle some of the different devices.

COMPUTER SYSTEMS GROUP 28

I. TIME-SHARED OPERATIONS

A. Capacity Improvements

In order to extract the maximum amount of computing power from the 360/67 central processing unit, expansions of main storage and access to input/output (I/O) units have been made during this quarter. To reduce the disk I/O bottleneck caused by queues of pending I/O requests, an additional channel was installed and the number of disk units on each channel was balanced. The elimination of queued I/O requests, which previously inhibited a user from obtaining system service, allows individual users as well as the system to achieve a greater I/O throughput. To obtain better CPU performance, an increase in the amount of core memory to 1.25 Mbytes was made. A decrease in wait time from 5 to 1 percent and a related decrease in supervisor time resulted in an increase in problem time for the CP/CMS time sharing system from 53 to 60 percent, or an increase in effective utilization of 13 percent. By dispatching more users in a given period of time, the system can be made more responsive or the total number of users can be increased. Since there is a demand for more time-sharing users, the maximum number of users was raised from 50 to 60. This number is not usually reached, partly because the number of terminals able to access the system is limited.

B. Graphics

To alleviate the problem of terminal access, preparations are being made for delivery of a programmable transmission control unit which will provide an increase in the number of ports by which terminals can access the time-sharing system. Since the new control unit will be programmable, it can be tailored to special Laboratory needs, such as providing a message switching facility or possibly performing the tasks of character translation. The initial objective is to provide a computer port for each terminal in the Laboratory, and in addition, to provide a capability for serving graphic terminals.

In order to provide an increased graphic capability for the 360/67, an experiment was performed using the ARPA network to send Stromberg-Datagraphics 4060 plotting data from the 360/67 time sharing system to the Terminal Support Processor (TSP) for display on a storage tube terminal. To improve the speed by which data are transmitted between a user program and the Network Control Program (NCP), which controls communications with the ARPA Network, a modification was made to CP-67 to provide for a virtual communications device that transfers data from one virtual machine to another through a core-core transfer facility. After the modifications were made, an increase in the speed of virtual machine communications from 128 to 5400 bytes/sec was obtained.

C. Upgraded CMS

Work on merging the Lincoln version of CMS, the time-sharing file system and command language, with the latest IBM version is progressing well. The file system in the new version

is ready for use and a number of command facilities have been updated for the merged system. What remains is to check out the language processors (FORTRAN and the Assembler) and their related execution time facilities. The new system will provide the ability to add to files or to write files in directories other than the user's primary directory. In addition, an improved OS SVC support package will enable more OS programs to run under CMS.

II. BATCH OPERATIONS

With the increase in main memory, a modified OS/360 batch processing system became operational. Modifications were made to the HASP job selection routine and to the OS core allocation routine. The standard job selection routine in HASP transfers jobs to OS for execution based solely on the number of active initiators (defined by the operator) and the order of the job classes on the initiators. For efficient core utilization, this scheme usually requires that the operator maintain careful control on the number of active initiators, the definition of the job classes on the initiators, and the number and order of the job classes read into the system. To minimize some of these operational considerations, the HASP selection routine was altered to include a check for core availability. That is, HASP will pass a job to OS only if the amount of core specified by the job's class is available. The order of the classes on the initiators is still significant since it continues to determine which job classes HASP will attempt to run first.

The OS core allocation routine was modified to allocate jobs requiring 300 K or less from the bottom, rather than the top, of core. This modification was made to prevent a core fragmentation problem from developing when processing jobs which require large amounts of core.

In other areas, a CMS program was coded to save on disk OS jobs submitted during the day. The program runs under the MONIT account and is activated every five minutes, at which time, any OS jobs read into CP for that account are written to disk. At the end of time sharing operations, the saved OS jobs are written on a tape which is subsequently read under OS. In 10 minutes, or less, all jobs are read into OS and ready for processing.

AIR TRAFFIC CONTROL DIVISION 4

INTRODUCTION

This section of the report reviews progress during the period 1 August through 31 October 1972 on Air Traffic Control projects funded by the Air Force. Separate reports describe the work of Division 4 on programs funded by the Federal Aviation Administration and Transportation Systems Center.

H. G. Weiss
Head, Division 4
P. R. Drouilhet
Associate Head

AIR TRAFFIC CONTROL

DIVISION 4

I. SUMMARY

The continuing studies related to proposed Microwave Landing Systems (MLS) are described. Recent work has focused upon multipath phenomena and the behavior of interferometer types of MLS. During this report period, a task was initiated for the Air Force Electronic Systems Division to provide experimental graphic display equipment for the SEEK BUS program. This experimental display will be installed in a C-131 aircraft currently equipped with a SEEK BUS terminal and will present command, control, navigation and traffic information to the pilot.

II. APPROACH AND LANDING SYSTEMS

Effort in support of the Laboratory's participation as the U.S. technical representative to the NATO Industrial Advisory Group (NIAG) Subgroup (SG-1) has been continuing. Subgroup 1 is in the process of assessing several alternative concepts for advanced approach and landing systems for the post-1975 period. Some of the concepts being assessed are being considered in the U.S. MLS program. There are, however, a variety of other concepts under consideration by NIAG SG-1 which are not part of the U.S. MLS program.

In recognition of the importance of coherent interference, i.e., multipath, and of efficient utilization of available RF spectrum, NIAG SG-1 has contracted with the Electronics Research Laboratory (ELAB) of the Norwegian Institute of Technology to assist in the assessment of these two critical areas. Lincoln Laboratory is participating in the "study control group" of SG-1 responsible for monitoring the ELAB contract. In support of this activity, Lincoln Laboratory has been assessing the multipath sensitivity of several of the alternative systems.

One issue that arises in assessing the multipath sensitivity of all concepts under consideration by SG-1 is the interplay between data rate* and multipath errors. We shall discuss this problem in a general framework and show that sampling theorem considerations suggest that systems with the higher data rate have a potential for better multipath rejection when other multipath rejection features, such as directivity, are equal. This potential is then examined at a specific airport (Runway 25R at Los Angeles International Airport) for three data rates:

- (a) 5 Hz - typical of mechanical scanning fan beams
- (b) 40 Hz - typical of "ground-derived" systems that perform direction finding on a DME interrogation
- (c) 1000 Hz - typical of a Doppler scanning system.

To expose the basic ideas, we shall consider the simple multipath situation shown in Fig. 1 for the case where a ground transmitted signal is analyzed aboard the aircraft, i.e., an

* By data rate, we mean here the rate at which the navigation system obtains data regarding the aircraft position as opposed to the rate at which it updates the position estimate furnished to the pilot and/or autopilot coupler.

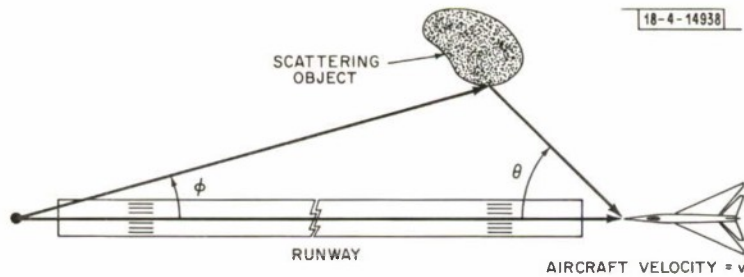


Fig. 1. Simple multipath reflection situation.

"air-derived" system (for a "ground-derived" system, one would reverse the direction of the arrows). If we define

ρ = ratio of reflection magnitude to direct path magnitude,

τ = time delay of reflection relative to direct path,

$\eta = 2\pi c \tau / \lambda$ = RF phase delay of reflection relative to direct path,

then the instantaneous error in aircraft azimuth due to multipath for each of the various systems is given by an equation of the form

$$e = f(\rho, \eta, \theta, \varphi) . \quad (1)$$

The functional form of f is, of course, different for each system due to antenna directivity, signal processing, etc.

We now note that as the aircraft moves along the flight path, the quantities ρ , η , θ and φ^* will change as a function of time. Thus, the error will be time varying. However, in most cases η varies much more rapidly than ρ , θ or φ . For example, if the reflection point does not change position too rapidly,

$$\frac{d\eta}{dt} \approx 2\pi \frac{v}{\lambda} (1 - \cos \theta) . \quad (2)$$

The dependence on η in Eq. (1) typically has a component sensitive to time delays on the order of the channel bandwidth and a second component which depends on η modulo 2π . The first component, for example, might correspond to the relation of the direct and multipath envelope, while the second corresponds to the relative RF phase difference. Consequently, the error in Eq. (1) is typically a periodic function of η with period 2π and an amplitude that varies slowly relative to the period; i.e., in time, the error is a periodic function with period

$$t_0 \approx \frac{\lambda}{v} (1 - \cos \theta) \quad (3)$$

whose amplitude varies slowly relative to t_0 . [This cyclic behavior has been termed "beam bends" in the current instrument landing system (ILS) literature.] Over time intervals where t_0 , ρ , θ and φ do not change significantly, the theory of Fourier series¹ tells us that $e(t)$ can be expanded as the sum of a set of sinusoids at frequencies $f_k = k/t_0$ with $k = 0, 1, 2, \dots$.

* φ changes because the specular reflection point will in general change.

We now wish to consider the potential for reducing this error via linear* receiver processing. If the data are received continuously, a low-pass filter can be used to reduce the multipath error at all frequencies above the minimum acceptable update rate. For example, the current ILS uses a filter with a time constant of 0.4 sec at its output,² so that the multipath error component at frequency f_k is attenuated by a factor of

$$G(f_k) = [(0.8\pi f_k)^2 + 1]^{-1/2} \quad (4)$$

If the data are now received at a rate R at discrete points in time, the ability to reduce multipath errors may be quite different from that suggested in Eq. (4), due to the interplay between the multipath frequencies and R . This is not due to practical compromises made in the receiver electronics, but rather, to a direct consequence of sampling theorem considerations.¹ This theorem states that if the Fourier transform of a function $g(t)$ is zero above a certain frequency W , then $g(t)$ can be uniquely determined from its values

$$g_n = g(n\pi/W)$$

at a sequence of equidistant points π/W apart. Conversely, if $g(t)$ is sampled at a rate R , then any frequency component of $g(t)$ at frequency $f > R$ is indistinguishable from components at frequency

$$f_{\text{alias}} = f - [f]_R \quad (5)$$

where $[\cdot]_x$ denotes modulo x [the term f_{alias} has been used for the quantity in Eq. (5), since this phenomenon is commonly referred to as "aliasing"]. Thus, for example, a sinusoid at 102.5 Hz sampled at 5 Hz cannot be separated from a sinusoid at 2.5 Hz on the basis of the sampled values alone.

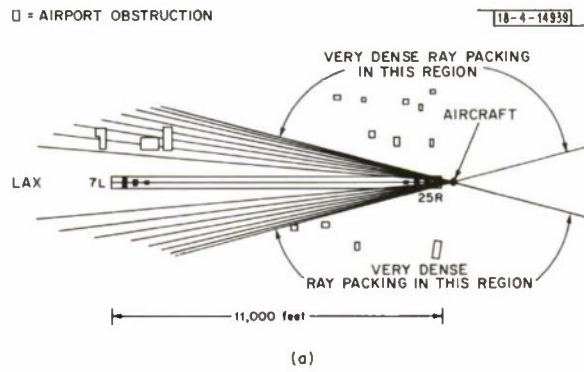
For an aircraft landing at 140 knots and having a C-band system ($\lambda = 0.2$ ft), Eq. (2) suggests that multipath frequencies as large as 2400 Hz can occur. We see from Eq. (4) that such frequency components would be heavily attenuated were the data provided continuously, but may be attenuated only slightly for the sampled data system if f_{alias} is close to zero (e.g., the sampled data attenuation using a 0.4 sec time constant is approximately $G(f) = [(0.8\pi f_{\text{alias}})^2 + 1]^{-1/2}$). From Eq. (2), we see that the angles Θ corresponding to $f \neq 0$ and $f_{\text{alias}} = 0$ are given by

$$\Theta_k = \cos^{-1}(1 - \frac{k\lambda R}{v}) \quad k = 1, 2, 3, \dots \quad . \quad (6)$$

In Figs. 2(a-c), we show the first few rays corresponding to Θ_k in Eq. (6) for an aircraft near threshold at Los Angeles International runway 25R for $R = 5, 40$ and 1000 Hz, respectively. In these figures, the points where a ray intersects an airport obstacle represent a situation where there will be little or no multipath rejection by low-pass filtering. Thus, we see that for this specific case, a 1000-Hz data rate system has a significantly greater potential for improving multipath performance by low-pass filtering.

* Keeping in mind the fact that if the error magnitude is very large, the receiver may utilize nonlinear processing to reduce the error (e.g., data from past observations are used to reject the data outright).

Division 4



(a)

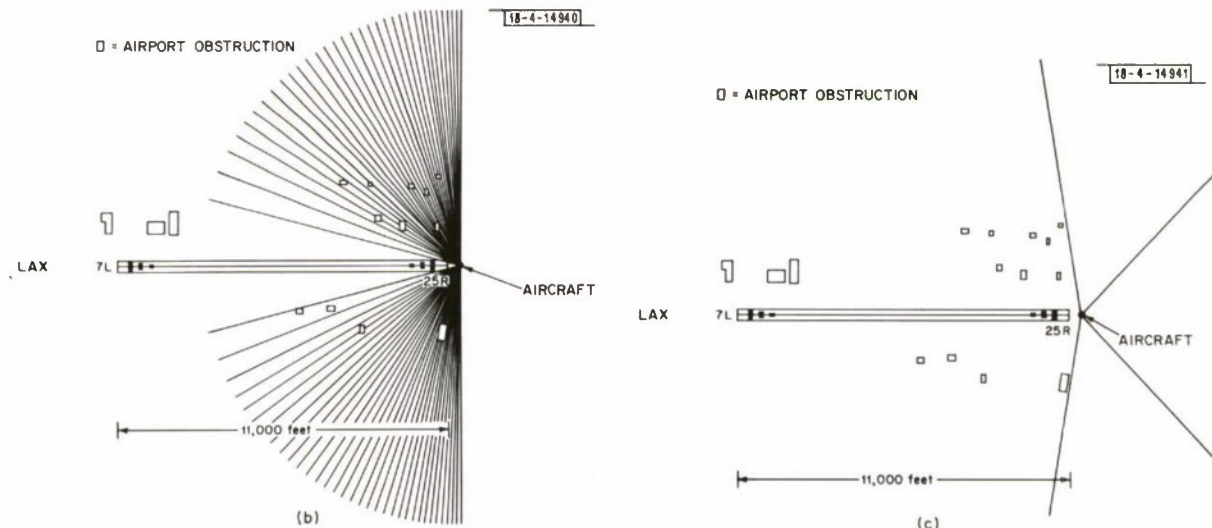


Fig. 2. Rays corresponding to zero alias frequency for (a) 5-Hz data rate; (b) 40-Hz data rate; and (c) 1000-Hz data rate.

A few observations are in order regarding the above results:

- (a) For ground reflection multipath at the usual glideslope angle of 2.5°, the angle Θ is very small so that the rate of change of η with time is quite slow.* In this case, no system will achieve significant improvement by low-pass filtering.
- (b) Specular reflection off airport obstructions, such as shown in Figs. 2(a-c), may be of sufficiently short duration relative to the aircraft dynamics that the additional multipath rejection via low-pass filtering is not needed.
- (c) A variety of issues must be considered in assessing the multipath induced error of various systems; hence, a high data rate system with the potential of improved low-pass averaging does not necessarily have better overall multipath rejection.
- (d) From Eqs. (2) and (4), we observe that the possible gain with low-pass filtering is a function of aircraft velocity. Thus, the tradeoff between data rate and typical obstruction locations must be performed anew for each potential application.

III. AIRBORNE GRAPHICAL DISPLAYS

The planning, design and construction of experimental airborne graphical display equipment for the SEEK BUS program is in progress. Lincoln Laboratory will provide this equipment and will evaluate its utility for presenting command and control, navigation and traffic data to a pilot. This airborne equipment is planned for installation in an Air Force C-131 aircraft that is currently equipped with a SEEK BUS airborne terminal. The graphical display will interface with existing equipment and will present to the pilot selected data transmitted from the 634B Technical Simulation and Evaluation Facility (TSEF) on the SEEK BUS data network.

Figure 3 shows an overall block diagram of the airborne graphical display system. The surveillance system is the TSEF and the data link is the SEEK BUS equipment. Airborne display equipment will process the received data and display only that information specifically selected by the pilot. The display computer will generate the appropriate alphanumeric tags for all traffic and map information. In addition, the computer will orient the map and target information with respect to the heading of the equipped aircraft while maintaining its position fixed in the center of the display.

Definitive specifications for the display package and the software have been prepared and construction and procurement activities are under way. The schedule is directed toward having equipment for installation in an aircraft by April 1973.

* If the aircraft-to-ground station distance x is very much greater than the aircraft height h_a and ground station height h_g , then

$$\frac{d\eta}{dt} \approx 4\pi \frac{h_a}{x} \cdot \frac{h_g}{x} v/\lambda = 4\pi \left(\frac{v}{\lambda}\right) (\text{glide slope angle}) \left(\frac{h_g}{x}\right)$$

since generally $h_g \ll h_a$, $(h_g/x) \ll$ glide slope angle and the frequency corresponding to this equation is quite low.

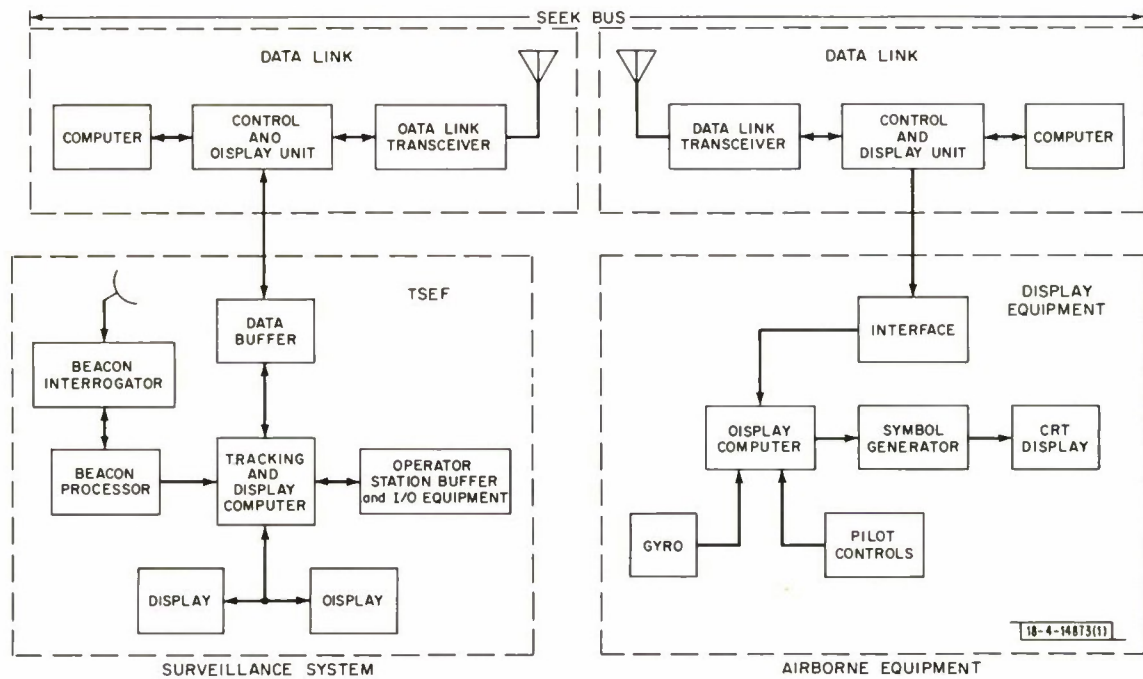


Fig. 3. Airborne graphical display system.

REFERENCES

1. A. Papoulis, The Fourier Integral and Its Applications (McGraw-Hill, New York, 1962).
2. RTCA Special Committee SC-79, "Standard Performance Criteria for Autopilot/Coupler Equipment," Radio Technical Commission for Aeronautics Paper 31-63/DO-118 (14 March 1963).

SOLID STATE DIVISION 8

INTRODUCTION

This section of the report summarizes progress during the period 1 August through 31 October 1972 on Solid State Research projects funded primarily by the Air Force. The Solid State Research Report for the same period describes this work of Division 8 in more detail.

A. L. McWhorter
Head, Division 8

P. E. Tannenwald
Associate Head

DIVISION 8 REPORTS ON ADVANCED ELECTRONIC TECHNOLOGY

15 August through 15 November 1972

PUBLISHED REPORTS

Journal Articles*

JA No.

3264	Magneto-Optical Properties	J. G. Mavroides	<u>Optical Properties of Solids</u> , F. Abeles, Ed. (North-Holland Publishing Co., Amsterdam, 1972), p. 355.
3857A	Comment on "Observation of Nonextremal Fermi Surface Orbita in Bulk Bismuth" — Author's Reply	V. E. Henrich	Phys. Rev. <u>B6</u> , 3151 (1972), DDC AD-752972.
3967	Sealed Crucible Technique for Thermal Analysis of Volatile Compounds up to 2500°C: Melting Points of EuO, EuS, EuSe and EuTe	T. B. Reed R. E. Fahey A. J. Strauss	J. Crystal Growth <u>15</u> , 174 (1972)
3970	Observation of Nuclear Hyperfine Splitting in the Infrared Vibration-Rotation Absorption Spectrum of the NO Molecule	F. A. Blum K. W. Nill A. R. Calawa T. C. Harman	Chem. Phys. Letters <u>15</u> , 144 (1972)
4018	High Resolution Spectroscopy Using Magnetic-Field-Tuned Semiconductor Lasers	K. W. Nill F. A. Blum A. R. Calawa T. C. Harman	Appl. Phys. Letters <u>21</u> , 132 (1972), DDC AD-752970.
4038	Tunable Infrared Laser Spectroscopy of Atmospheric Water Vapor	F. A. Blum K. W. Nill P. L. Kelley A. R. Calawa T. C. Harman	Science <u>177</u> , 694 (1972), DDC AD-752998.
4045	NaYF ₄ :Yb, Er — An Efficient Upconversion Phosphor	N. Menyuk K. Dwight J. W. Pierce	Appl. Phys. Letters <u>21</u> , 159 (1972), DDC AD-752985.
4049	The Effect of Inhomogeneities in Acoustic-Surface-Wave Amplification	B. E. Burke Abraham Bers†	Appl. Phys. Letters <u>21</u> , 449 (1972)

* Reprints available.

† Author not at Lincoln Laboratory.

Division 8

JA No.

4053	Collisional Narrowing of Infrared Water-Vapor Transitions	R. S. Eng A. R. Calawa T. C. Harman P. L. Kelley A. Javan*	Appl. Phys. Letters <u>21</u> , 303 (1972), DDC AD-753003.
4071	Double-Heterostructure GaAs:Si Diode Lasers	J. A. Rossi J. J. Hsieh	Appl. Phys. Letters <u>21</u> , 287 (1972), DDC AD-753005.
4072	Submillimeter Spectroscopy	H. R. Fetterman H. R. Schlossberg* J. Waldman	Laser Focus <u>8</u> , 42 (1972), DDC AD-753006.
4106	Identification of Donor Species in High-Purity GaAs Using Optically Pumped Submillimeter Lasers	H. R. Fetterman J. Waldman C. M. Wolfe G. E. Stillman C. D. Parker	Appl. Phys. Letters <u>21</u> , 434 (1972)

Meeting Speeches

MS No.

3090	Influence of Madelung Energy and Covalency on the Structure of $A^+B^{5+}O_3^-$ Compounds	J. A. Kafalas	Solid State Chemistry, <u>Proceedings of 5th Materials Research Symposium</u> , R. S. Roth and S. J. Schneider, Eds. (N. B. S. Special Publication 364, July 1972), p. 287
3120	Preparation and Structure of a Pyrochlore and Perovskite in the $BiRhO_{3+x}$ System	J. M. Longo P. M. Raccah J. A. Kafalas J. W. Pierce	Solid State Chemistry, <u>Proceedings of 5th Materials Research Symposium</u> , R. S. Roth and S. J. Schneider, Eds. (N. B. S. Special Publication 364, July 1972), p. 219

* * * * *

UNPUBLISHED REPORTS

Journal Articles

JA No.

4036	Ferromagnetism	J. B. Goodenough	Accepted by <u>Encyclopedia of Chemistry</u> (Utet/Sansoni Edizioni Scientifiche, Firenze)
4043	Giant Quantum Oscillations in High Purity Bismuth: Search for Hole Fermi Surface Anomalies	V. E. Henrich	Accepted by Phys. Rev.
4068	Two-Phonon Deformation Potential	K. L. Ngai* E. J. Johnson	Accepted by Phys. Rev. Letters

* Author not at Lincoln Laboratory.

JA No.

4081	Electric Field Induced Transient Spin-Flip Raman Laser Pulses in InSb	A. Mooradian S. R. J. Brueck E. J. Johnson J. A. Rossi	Accepted by Appl. Phys. Letters
4083	Submillimeter Lasers Optically Pumped off Resonance	H. R. Fetterman H. R. Schlossberg* J. Waldman	Accepted by Optics Commun.
4087	PbS Photodiodes Fabricated by Sb ⁺ Ion Implantation	J. P. Donnelly T. C. Harman A. G. Foyt W. T. Lindley	Accepted by Solid State Electronics
4089	Exciton Levels in a Magnetic Field	N. Lee* D. M. Larsen B. Lax*	Accepted by J. Phys. Chem. Solids
4094	Theory of the Spontaneous Spin-Flip Raman Lineshape in InSb	R. W. Davies	Accepted by Phys. Rev.
4097	High Resolution Photoconductivity Studies of Residual Shallow Donors in Ultrapure Ge	S. D. Seccombe D. M. Korn	Accepted by Solid State Commun.
4107	Procedure for Polishing PbS and PbS _{1-x} Se _x	G. A. Ferrante M. C. Lavine T. C. Harman J. P. Donnelly	Accepted by J. Electrochem. Soc.
4115	Anomalously High "Mobility" in GaAs	C. M. Wolfe G. E. Stillman D. L. Spears D. E. Hill* F. V. Williams*	Accepted by J. Appl. Phys.
4116	Growth of Crystals of V ₂ O ₃ and (V _{1-x} Cr _x) ₂ O ₃ by the Tri-Arc Czochralski Method	J. C. C. Fan T. B. Reed	Accepted by Mater. Res. Bull.
MS-3338	Stripe-Geometry Pb _{1-x} Sn _x Te Diode Lasers	R. W. Ralston I. Melngailis A. R. Calawa W. T. Lindley	Accepted by IEEE J. Quantum Electron.
MS-3344	Photothermal Ionization of Shallow Donors in GaAs	G. E. Stillman C. M. Wolfe D. M. Korn	Accepted by Proc. 11th Intl. Conf. on the Physics of Semiconductors, Warsaw, Poland, 25-29 July 1972
MS-3350	Small Bandgap Lasers and Their Uses in Spectroscopy	A. R. Calawa	Accepted by Proc. C. S. A. T. A. Symp. on "The Physics and Technology of Semiconductor Light Emitters and Detectors," Pugnochiuso, Italy, 4-10 September 1972
MS-3351	Small Bandgap Semiconductor Infrared Detectors	I. Melngailis	

* Author not at Lincoln Laboratory.

Division 8

<u>JA No.</u>			
MS-3353	Dependence of Growth Temperature on Carrier Gas Velocity in Open Tube Transport	T. B. Reed W. J. LaFleur	Accepted by J. Crystal Growth
MS-3367	Pseudobinary Phase Diagram and Existence Regions for $\text{PbS}_{1-x}\text{Se}_x$	A. J. Strauss T. C. Harman	Accepted by J. Electronic Materials
MS-3369A	Proton Guarded GaAs IMPATT Diodes	R. A. Murphy W. T. Lindley D. F. Peterson A. G. Foyt C. M. Wolfe C. E. Hurwitz J. P. Donnelly	Accepted by Proc. 4th Intl. Symp. on GaAs and Related Compounds, Boulder, Colorado, 25-27 September 1972
MS-3373	The Structure of La_2CuO_4 and LaSrVO_4	J. M. Longo P. M. Raccah	Accepted by J. Solid State Chem.
MS-3391	Narrow-Gap Semiconductor Lasers and Detectors	I. Melngailis	Accepted by Proc. 1972 Conf. on Solid State Devices, Tokyo, Japan, 30-31 August 1972
MS-3392	Schottky Barrier GaAs Electron Beam Semiconductor Amplifier (EBIRD)	W. T. Lindley W. E. Krag C. M. Wolfe R. J. Sasiela R. A. Murphy C. E. Hurwitz D. F. Kostishack A. J. Yakutis A. G. Foyt	Accepted by Proc. 4th Intl. Symp. on GaAs and Related Compounds, Boulder, Colorado, 25-27 September 1972

Meeting Speeches*

<u>MS No.</u>			
3090A	High Pressure Synthesis	J. A. Kafalas	Dept. of Chemistry Seminar, Yeshiva University, New York, New York, 18 October 1972
3248	High Resolution Spectroscopy in the $5 \mu\text{m}$ Region Using Tunable Semiconductor Lasers	F. A. Blum K. W. Nill	Gordon Research Conference on Infrared Spectroscopy, Meriden, New Hampshire, 14-18 August 1972
3318C	High Resolution Infrared Spectroscopy Using Tunable Semiconductor Lasers	K. W. Nill F. A. Blum	4th Northeast Regional Meeting, American Chemical Society, Hartford, Connecticut, 18 October 1972
3337A	Tunable Semiconductor Lasers	A. Mooradian	Gordon Research Conference on Infrared and Raman Spectroscopy, Meriden, New Hampshire, 14-18 August 1972

* Titles of Meeting Speeches are listed for information only. No copies are available for distribution.

MS No.

3337B	Tunable Semiconductor Lasers	A. Mooradian	Seminar, Lawrence Livermore Laboratory, University of California, Livermore, California, 21 August 1972
3337C	Tunable Semiconductor Lasers	A. Mooradian	IEEE Seminar, Tufts University, Medford, Massachusetts, 17 October 1972
3337D	Tunable Semiconductor Lasers and Their Applications	A. Mooradian	Seminar on Laser Technology, George Washington University, Washington, D.C., 19 October 1972
3345	An Integrated Intermediate Frequency Amplifier-Limiter	J. K. Roberge* W.H. McGonagle	1972 Government Microcircuit Applications Conference, San Diego, California, 10-12 October 1972
3350	Small Bandgap Lasers and Their Uses in Spectroscopy	A. R. Calawa	C.S.A.T.A. Symp. on "The Physics and Technology of Semiconductor Light Emitters and Detectors," Pugnochiuso, Italy, 4-10 September 1972
3351	Small Bandgap Semiconductor Infrared Detectors	I. Melngailis	C.S.A.T.A. Symp. on "The Physics and Technology of Semiconductor Light Emitters and Detectors," Pugnochiuso, Italy, 4-10 September 1972
3367	Pseudobinary Phase Diagram and Existence Regions for $\text{PbS}_{1-x}\text{Se}_x$	A.J. Strauss T.C. Harman	Electronic Materials Conference, Boston, Massachusetts, 28-30 August 1972
3369A	Proton Guarded GaAs IMPATT Diodes	R. A. Murphy W. T. Lindley D. F. Peterson A. G. Foyt C. M. Wolfe C. E. Hurwitz J. P. Donnelly	4th Intl. Symp. on GaAs and Related Compounds, Boulder, Colorado, 25-27 September 1972
3373	The Structure of La_2CuO_4 and LaSrVO_4	J. M. Longo P. M. Raccah	Northeastern Regional Meeting, American Chemical Society, New York, New York, 27 August - 1 September 1972
3374	Preparation of Infrared-to-Visible Upconversion Phosphors Based on Hexagonal NaYF_4	J. W. Pierce E. J. Delaney K. Dwight N. Mcnyuk	

* Author not at Lincoln Laboratory.

Division 8

MS No.

3391	Narrow-Gap Semiconductor Lasers and Detectors	I. Melngailis	1972 Conf. on Solid State Devices, Tokyo, Japan, 30-31 August 1972
3392	Schottky Barrier GaAs Electron Beam Semiconductor Amplifier (EBIRD)	W. T. Lindley W. E. Krag C. M. Wolfe R. J. Sasiela R. A. Murphy C. E. Hurwitz D. F. Kostishack A. J. Yakutis A. G. Foyt	4th Intl. Symp. on GaAs and Related Compounds, Boulder, Colorado, 25-27 September 1972
3407	Use of Tunable Semiconductor Lasers in High Resolution Infrared Spectroscopy Near 5 μm	K. W. Nill F. A. Blum	"Tunable Lasers" Conference, Heriot-Watt University, Edinburgh, Scotland, 6-8 September 1972
3412	High Frequency Surface Wave Transducers Fabricated by X-Ray Lithography	D. L. Spears H. I. Smith	IEEE Ultrasonics Symp., Boston, Massachusetts, 4-6 October 1972
3415	High Resolution Molecular Spectroscopy Near 5 μm Using Tunable Semiconductor Lasers	F. A. Blum K. W. Nill A. R. Calawa T. C. Harman	1st International Conference on Spectral Lines, Knoxville, Tennessee, 28 August - 1 September 1972
3455	Ion Implantation and Some Applications to Compound Semiconductor Devices	J. P. Donnelly	Colloquium, Division of Electrical Engineering and Applied Physics, Case Western Reserve University, Cleveland, Ohio, 2 November 1972
3459	High Resolution Photoconductivity Studies of Residual Shallow Donors in Ultrapure Germanium as Studied by Fourier Transform Spectroscopy	D. M. Korn	Physics Seminar, 3M Central Research Laboratory, St. Paul, Minnesota, 10 November 1972

SOLID STATE DIVISION 8

I. SOLID STATE DEVICE RESEARCH

Linear arrays of 20 closely spaced InSb n-p junction photodiodes have been fabricated using the techniques of proton bombardment and field plate guarding. These arrays exhibit good elemental detector performance as well as excellent uniformity among elements of an array. The variation in the detectivity of the elements in an array was measured to be less than 10 percent. In addition, the yield of good arrays per wafer has been unusually high. Out of 50 arrays fabricated on a single wafer, only seven arrays had defective diodes.

Using Sb⁺ ion implantation to create the n-type layer, n-p junction photodiodes in PbS have been fabricated. The Sb⁺ implantation process is similar to that previously used in the fabrication of bulk PbTe photodiodes. The zero-bias resistance for the 15-mil-square PbS diodes was typically 200 ohms at 300°K, 5×10^4 ohms at 195°K, and 5×10^9 ohms at 77°K. Peak detectivities occurred at 2.55, 2.95 and 3.4 μm at 300°, 195° and 77°K, respectively. The corresponding measured detectivities were 4.8×10^9 , 1.1×10^{11} and 4.2×10^{12} cmHz^{1/2}/W. The 77°K detectivity was measured in a reduced background and was amplifier noise limited. Peak quantum efficiencies were typically 50 to 60 percent.

Similar Sb⁺ ion implants into PbTe films which have been grown epitaxially on BaF₂ substrates have also yielded high quality n-p photodiodes. At 77°K, a typical 15-mil-square photodiode had a zero-bias resistance of 1 megohm, a peak detectivity of 4.5×10^{11} cmHz^{1/2}/W at 5.3 μm and a quantum efficiency of 55 percent.

The thermal properties of PbS_{1-x}Se_x diode lasers with n-p junctions formed by Sb⁺ ion implantation have been studied by observing the temperature tuning of the laser frequency for a number of different operating conditions. The continuous DC tuning rate was measured as a function of current in CW operation, the thermal response was determined by applying a small-amplitude AC current to a DC-biased laser, and the laser frequency chirp rate was measured under pulsed conditions.

II. QUANTUM ELECTRONICS

Using an optical parametric oscillator as an optical pump, peak powers on the order of one watt and conversion efficiencies of 3 to 4 percent have been obtained from InP and In_xGa_{1-x}As semiconductor lasers. Tuning of the pump allows bulk optical excitation, thus reducing surface recombination and spreading the heat load.

Gallium arsenide diode lasers operating at 77°K have been hydrostatic pressure tuned in the 0- to 7-kbar range and their spectral characteristics have been studied. Time resolved spectroscopy has been carried out on Cs¹³³ using the frequency swept output of a pulsed laser. Sufficient resolution is obtained for Doppler-limited spectroscopy.

Small signal gain measurements have been made on the spin-flip Raman laser by observing the amplification of a second CO laser line at a frequency lower than the pump line. Measurements of the Raman gain profile were made by tuning the spin-flip frequency through the frequency

Division 8

difference between the CO laser lines. By observing the gain profile at a number of CO line separations the dependence of linewidth on magnetic field was determined. Four wave mixing processes were also seen.

III. MATERIALS RESEARCH

The pseudobinary phase diagram of the PbS-PbSe system has been re-determined by using thermal analysis to measure the liquidus temperatures and electron microprobe analysis of Bridgman-grown ingots to establish the solidus points. The chalcogen-rich solidus lines for PbS and $\text{PbS}_{0.62}\text{Se}_{0.38}$ have been determined by means of Hall coefficient measurements on samples that were chalcogen-saturated by isothermal annealing and then quenched.

It has been demonstrated that the composition of $\text{PbS}_{1-x}\text{Se}$ alloys can be conveniently and rapidly determined by using x-ray fluorescence to measure their Se content. A calibration curve was established by measurements on samples whose compositions had been determined by electron microprobe analysis.

IV. PHYSICS OF SOLIDS

In the continuing rare-earth phosphor upconversion program, a study has been carried out of the $\text{NaYF}_4\text{:Yb, Tm}$ anti-Stokes emission ($\approx 0.81 \mu\text{m}$) which is of interest because it matches the absorption band of YAG:Nd. The onset of saturation effects in the phosphor appears to make the combination of a GaAs:Si diode with the phosphor less efficient than a GaAsP diode for pumping a YAG:Nd laser.

In one phase of the secondary electron emission program, the search for materials with high yields at low primary electron energies has turned to mixtures of insulating and conducting particles where the individual grains are small enough to allow tunneling to the conducting regions. Au-MgO films produced by sputtering look promising, and detailed studies of the effects on the yield of conducting and insulating substrates, substrate temperature, annealing and composition are now being carried out.

The free energy model, developed earlier for the insulator-metal transition in Ti_2O_3 , has been extended to describe the high temperature transition in V_2O_3 . A series of curves has been calculated which agrees qualitatively with the temperature dependence of the c-axis parameter observed in a series of Cr-doped V_2O_3 samples.

Work on high resolution laser spectroscopy on NO continues. The Zeeman spectra of the $\text{Q}(3/2)_{3/2}$ and $\text{Q}(5/2)_{3/2}$ absorption lines, obtained by tuning these lines into coincidence with the $\text{P}(15)_{9,8}$ emission line of a CO gas laser, exhibit fine structure, much larger than that expected by present theory and the known molecular constants of NO. In other work, a current-tuned, lead-salt diode laser was used to study the R branch of NO at 77°K where nuclear hyperfine structure, obscured at room temperature because of Doppler broadening, is observed and found to be consistent with theory.

V. MICROELECTRONICS

At intervals, as has been done in the past, it seems appropriate to provide a general review of the overall Microelectronics Program. In addition to several major programs such as Electron Beam Semiconductor development, LES IMPATT diode packaging, special mirror development,

and sputtered metal oxide processing, there is preliminary development work in such areas as optoelectronic semiconductors, nuclear particle detector arrays and charge coupled devices.

The service base for routine work has increased slightly during this past quarter and about 50 work orders for thin film deposition, bonding and assembly, and other processing have been undertaken. Some of these requests involved routine processing of a number of pieces, while other requests required special processing of one or two parts.

The mask making for various laboratory programs continues at a relatively high level with 280 masks delivered during this quarter.

UNCLASSIFIED

Security Classification

DOCUMENT CONTROL DATA - R&D

(Security classification of title, body of abstract and indexing annotation must be entered when the overall report is classified)